Available online at www.sciencedirect.com
SCIENCE DIRECT
Electrochemistry Communications 8 (2006) 1292–1298
electrochemistry communications
www.elsevier.com/locate/elecom

On-demand design of polyoxianionic cathode materials based on electronegativity correlations: An exploration of the Li_2MSiO_4 system (M = Fe, Mn, Co, Ni)

M.E. Arroyo-de Dompablo [a,*], M. Armand [b], J.M. Tarascon [b], U. Amador [c]

[a] Departamento de Química Inorgánica, Facultad de CC. Químicas, Universidad Complutense de Madrid, 28040 Madrid, Spain
[b] LRCS, Université de Picardie Jules-Verne, UMR 6007 CNRS, 33 rue Saint-Leu, 80039 Amiens, France
[c] Departamento de Química, Universidad San Pablo-CEU, 28668-Boadilla del Monte, Spain

Received 7 May 2006; accepted 5 June 2006
Available online 10 July 2006

Abstract

A first principles investigation is performed to quantify how the inductive effect of different polyoxianions $(XO_4)^{n-}$ (X = Ge, Si, Sb, As, P) affects the lithium deintercalation voltage of olivine-$LiCo^{+2}XO_4$, $Li_yV^{+4}OXO_4$ and $Li_yM^{+2}XO_4$ (M = Mn, Fe, Co, Ni within the structure of Li_2FeSiO_4) compounds. In all cases, the calculated lithium deintercalation voltage correlates to the Mulliken X electronegativity, displaying a linear dependence for each *structural type/redox couple*. Experimental lithium deinsertion voltages already available in the literature support these results. Computational results on Li_2MSiO_4 are used to evaluate the electrochemical performance of these materials. Li_2FeSiO_4 will develop a reversible specific capacity limited to the extraction of one lithium ion. Li_2MnSiO_4 is predicted to have a poor electronic conductivity. The calculated lithium extraction voltages of Co and Ni silicates are too high for current electrolytes. The optimized structure of the fully delithiated $MSiO_4$ suggests that this host is unstable, pointing out to a possible structural transformation during the charge/discharge of the lithium cells.

Keywords: Silicates; Electrode material; Li-ion battery; Electronegativity; Density functional theory

1. Introduction

Goodenough et al. put forward, for polyoxianionic structures possessing M–O–X bonds, the possibility to change the iono-covalent character of the M–O bonding through inductive effect by selecting different X elements, so as to establish a systematic mapping and tuning of transition-metal redox potentials [1–3]. An extensive compendium of lithium intercalation voltage shifts in polyoxioanionic compounds owed to the inductive effect can be found [4]. Though the role of the "inductive effect" on the electrochemistry of polyoxianionic compounds is qualitatively well understood, a quantitative correlation of Li intercalation voltages to the inductive effect is missing to date. The first aim of this work is to provide precise values of lithium intercalation voltage variations occurring within polyoxianionic compounds due to the inductive effect of different oxoanion groups (XO_4^{n-}; X=P, Si, Ge, etc.) as a result of different X-electronegativities. Such voltage-electronegativity correlations would be quite useful to propose novel electrode materials.

The inductive effect is the polarization of the M–O chemical bond caused by the polarization of the adjacent X–O bond. Hence, one could expect that in polyoxianionic structures possessing M–O–X bonds, the X electronegativity determines the polarization of the X–O bond, and consequently the iono-covalent character of the M–O bond. Within this scenario, we postulated that in these compounds the lithium intercalation voltage should correlate to the X electronegativity. Indeed, recently, a combination of experimental and computational methods showed that

* Corresponding author. Tel.: +34 91 3945168; fax: +34 91 3944352.
E-mail address: e.arroyo@quim.ucm.es (M.E. Arroyo-de Dompablo).

1388-2481/$ - see front matter © 2006 Elsevier B.V. All rights reserved.
doi:10.1016/j.elecom.2006.06.003

the evolution of V–O distances, electronic band-gaps and lithium intercalation voltages in Li_yVOXO_4 (V^{+4}/V^{+5} redox couple with X = Ge, Si, As, P and their mixtures) correlate to the X Mulliken electronegativity [5–7]. The linear dependence of lithium intercalation voltages with the X electronegativity observed in Li_yVOXO_4 leads to the concept of "data transferability" in polyoxianionic compounds within a given structural type and for a particular redox couple. In this work, we investigate from first principles calculations whether such Li insertion voltage-X electronegativity correlation is a general feature of polyoxianionic compounds, thereby existing in other structures and/or with other redox couples. To do so, we have completed previous studies on olivine-$LiCoXO_4$ [8] and extend the investigation to the Li_yMXO_4 compounds (M = Mn, Fe, Co, Ni; X = P, Si, Ge; $y = 1, 2$) possessing the Li_2FeSiO_4 structure.

The use of Li_2MSiO_4 as cathode materials was suggested as early as 1997 in the wake of the emergence of the phosphate electrode [9]. The electrochemistry of Li_2FeSiO_4, Li_2FeGeO_4 and L_2MnSiO_4 towards Li^+/Li has been reported since showing that these compounds are able to provide one electron per formula unit at average voltages of *ca.* 3.1 V, 3.05 V and 4.2 V, respectively [10,11]. Yang et al. succeeded to remove the two lithiums from Li_2MnSiO_4[12], though the electrode suffers a large polarization. Along these lines we show that in Li_yMXO_4 (X = Ge, Si, P; M = transition metal; $y = 1,2$) compounds lithium intercalation voltages and band-gaps correlate to the X electronegativity. Thus, as a second goal, we will use this correlation between X electronegativity and band-gaps and lithium insertion voltage in the family of compounds derived from Li_2FeSiO_4 in an attempt to design better silicates $Li_2MSi_{1-y}X_yO_4$ of potential interest as electrode for Li-ion batteries.

1.1. Structures

A computational investigation requires as only inputs the structure and composition of a material, hence making it possible the study of hypothetical compounds, even in the case that for a given composition (and thermodynamic conditions) the material is known to occur as a different polymorph. For instance, one can compute the lithium insertion voltage of olivine-$LiCoSbO_4$, though the compound forms a spinel structure [13]. Results on hypothetical compounds are quite useful to confirm hypotheses extracted from the study of existing compounds. In this work three families of compounds have been investigated: the aforementioned Li_yMOXO_4 (M = V), olivine-$LiMXO_4$ (M = Co) and the Li_yMXO_4 (M = Mn, Fe, Co, Ni). For each of these materials we have studied hypothetical as well as existing compounds.

The structure of Li_2VSiO_5 is built up from $[VOSiO_4]_2$-layers of VO_5 square pyramids sharing corners with SiO_4 tetrahedra, and intercalated with Li ions [14]. In the olivine ($LiMXO_4$) structure the MO_6octahedra share four corners in the ***cb***-plane being bridged along the ***a***-axis by the XO_4 groups, whereas the Li ions are located in rows, running along ***a***, of edge-sharing LiO_6 octahedra that appear between two consecutive $[MO_6]_\infty$ layers. The structure of Li_2FeSiO_4 (Fig. 1) can be described as built up from infinite corrugated layers of composition $[SiFeO_4]_\infty$ lying on the ***ac***-plane and linked along the ***b***-axis by LiO_4 tetrahedra. Within these layers each SiO_4 tetrahedron shares its four corners with four neighboring FeO_4 tetrahedra, and vice versa. Lithium ions also occupy tetrahedral sites located between two of the $[SiFeO_4]_\infty$ layers, in such a way that three of the oxygen atoms of every LiO_4 tetrahedra belong to the same layer and the fourth one to an adjacent layer. A path for lithium motion (facilitating the extraction/insertion process) exists in the structure since the LiO_4 tetrahedra are arranged in rows running along the ***a***-axis by corner-sharing. These structures are determined by the environment adopted by the transition metal ions: square pyramidal in Li_yVOXO_4, octahedral in olivine-$LiCoXO_4$, and tetrahedral in Li_yMXO_4. To sweep the electronegativity scale, as central atoms of the XO_4 groups we selected Ge (1.95), Sb (2.06), Si (2.03), As (2.26) and P (2.39). Throughout this work we will refer to Mulliken electronegativities given in Pauling units (data taken from Allen [15]).

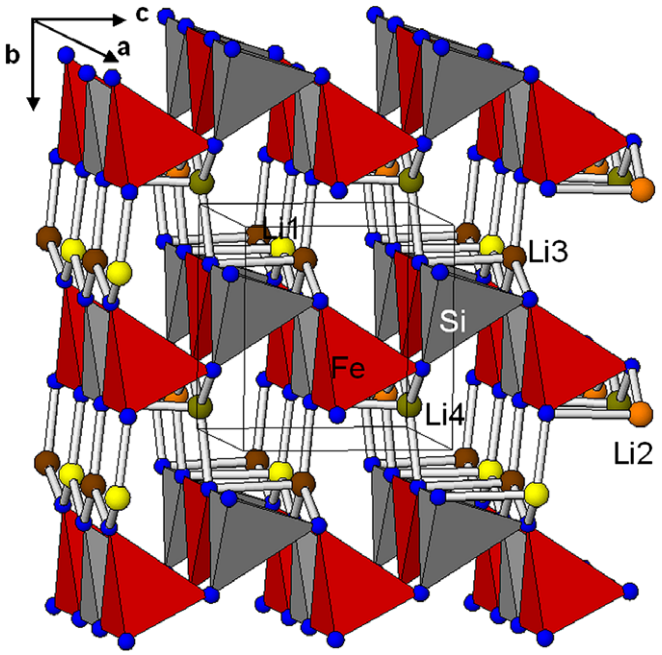

Fig. 1. Schematic crystal structure of optimized-Li_2FeSiO_4. Li ions at sites 1, 2, 3 and 4 are labeled and colored differently.

2. Methodology

The total energies of all the compounds under study were calculated using the Projector Augmented Wave (PAW) [16,17] method as implemented in the Vienna *ab initio* simulation package (VASP)[18]. The exchange and correlation energies have been approximated in the Generalised Gradient Approximation with the Hubbard parameter correction (GGA + *U*). Computational details

for Li_2VXO_5 [5,7] and $LiCoXO_4$ [8] are provided elsewhere. For the Li_2MXO_4 compounds a J correction term of 1 eV was used, with a U value of 6 eV (M = Mn, Co and Ni) and 5 eV (M = Fe), in accordance with previous DFT + U investigations [19,20]. To asses this choice we calculated the lithium deinsertion voltage from Li_2FeSiO_4 for different U values, obtaining voltages of 3.29 V, 3.16 V, 3.02 V, 2.89 V for $U = 6$ eV, 5 eV, 4 eV and 3 eV, respectively, while the pure GGA gives a voltage of 2.59 V. For Li_2MnSiO_4 calculated lithium deinsertion voltages are 4.33 V, 4.13 V, and 3.92 V for $U = 6$ eV, 5 eV and 4 eV, respectively. The energy cut off for the plane wave basis set was kept at a constant value of 500 eV and the reciprocal space sampling done with k-point grids of $4 \times 4 \times 4$. The initial cell parameters and atomic positions were taken from those reported by Nytèn et al. [11] for Li_2FeSiO_4. From the fully relaxed structures, Li ions were removed leading to "$LiMSiO_4$" and "$MSiO_4$" compounds (see results for details on delithiated structures) which were also fully relaxed. In all cases the final energies of the optimized geometries were recalculated so as to correct for changes in basis during relaxation. Lithium intercalation voltages have been calculated following the methodology described by Aydinol et al. [21].

3. Results

3.1. Voltage and band-gap correlations to X electronegativity

We have computed the lithium insertion voltage of the following reactions:

$$Co^{+3}XO_4 + Li \leftrightarrow LiCo^{+2}XO_4 \quad (X = P, As, Sb) \tag{1}$$

$$Li_yV^{+5}OXO_4 + Li \leftrightarrow Li_{y+1}V^{+4}OXO_4 \quad (X = P, As, Si, Ge) \tag{2}$$

$$Li_yM^{+3}XO_4 + Li \leftrightarrow Li_{y+1}M^{2+}XO_4 \quad (M = Mn, Fe, Co, Ni \text{ and } X = P, Si, Ge) \tag{3}$$

The crystalline structures of delithiated phases in reactions (1) and (2) are known [5,8]. When removing lithium ions from Li_2MSiO_4 (reaction (3)), different lithium-vacancy arrangements could be considered at the composition $LiMSiO_4$. Among the numerous possible arrangements structures were chosen so as to have the smallest unit cell. Hence, from Li_2MSiO_4 lithium ions were selectively removed, with the remaining lithium ions at sites 1 and 2 (A), 1 and 3 (B) and 2 and 3 (C). The ordered structure with the lowest total energy for M = Fe, Co and Ni is C; the most unstable structure (B) being, respectively, 0.24 eV, 0.22 eV and 0.19 eV higher in energy. In the case of $LiMnSiO_4$, structure A appeared to be 0.013 eV lower in energy than structure C, and 0.17 eV lower than structure B. Since the energy difference between A-Li_2MnSiO_4 and C-Li_2MnSiO_4 is small for the purpose of this work, and for a shake of simplicity, thereafter, we will refer solely to $LiMXO_4$ compounds possessing the structure C.

Fig. 2 plots the calculated lithium insertion voltage for reactions (1)–(3) as a function of the X Mulliken electronegativity in Pauling units. Available experimental data (crosses) are provided for comparison; the computational method reproduces the experimental lithium insertion voltage of any compound with errors below 0.15 V. In all cases, the voltage increase with the electronegativity of X displays an almost a linear dependence. As expected, the TM ion has the major effect over the voltage. In the Li_yMXO_4 ($y = 2$ or 1) compounds, with the Li_2FeSiO_4 or the partially deinserted □$LiFeSiO_4$ structures, moving from one TM ion to other it is possible to sweep a wide voltage range, between 4.8 V in hypothetical $LiNiPO_4$ (purple line) and 3.15 V in Li_2FeGeO_4 (orange line). For a same redox couple (Co^{+2}/Co^{+3}) the effect of structure on the lithium insertion voltage spans 0.3 V as observed when comparing olivine-$LiCoPO_4$ (red) to the hypothetical-$LiCoPO_4$ with the □$LiFeSiO_4$ structure (dark yellow). For a given structure-couple the maximum voltage difference in the investigated X-electronegativity range is of 0.4 V in the V^{+4}/V^{+5} redox couple (compare Li_2VOGeO_4 with $LiVOPO_4$). Interestingly, the slope of the voltage–electronegativity linear functions seems to be affected by the environment of the TM ions.

Information on intrinsic electronic conductivity (band-gaps) can be deduced from the calculated density of states of the compounds under investigation. Though quantitative band-gaps in the GGA + U method are known to be dependent on the value of the U parameter [5,20,22,23], reliable general trends can be extracted from such DOS calculation. Fig. 3 shows the calculated band-gap as a function of the X electronegativity for the reduced forms of reactions (1)–(3). Generally speaking, no evident correlation between the band-gap of reduced compounds and the electronegativity is observed. In most cases silicates and phosphates have similar band-gaps. A carefully observation suggests that the band-gap decreases the heavier the X atoms down in a column of the Periodic Table (see for instance evolution in olivine-$LiCo^{+2}XO_4$). However, caution should be exercised when relating calculated band-gaps to electronic conductivities. Band-gaps solely provide information of the intrinsic electronic conductivity of a

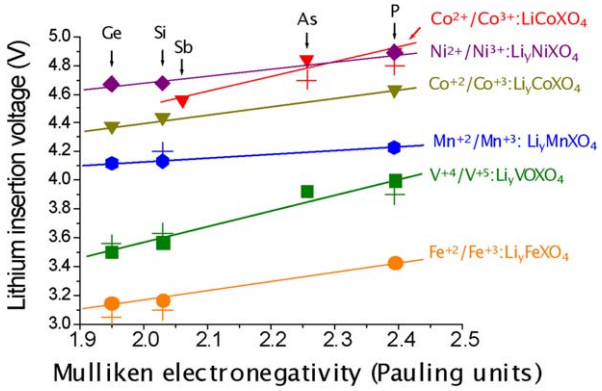

Fig. 2. Calculated and experimental (crosses) lithium insertion voltage for polyoxianionic compounds *vs.* the X Mulliken electronegativity. The lines show the fit to respective linear functions.

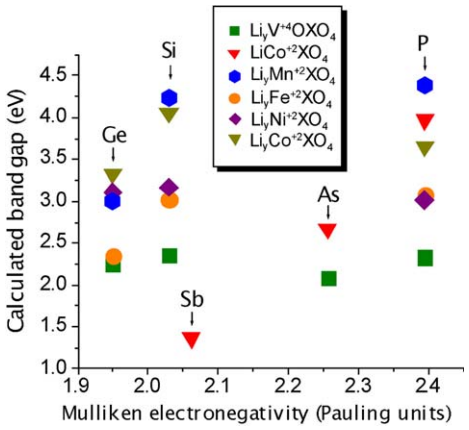

Fig. 3. Calculated band-gaps for $LiCo^{+2}XO_4$, $Li_yV^{+4}OXO_4$ and $Li_yM^{+2}XO_4$ compounds *vs.* the X Mulliken electronegativity.

material due to the thermal excitation of delocalized electrons across the gap, but other conduction mechanisms might exist, as observed in olivine-$LiFePO_4$ where the conductivity occurs through localized polarons [20,24].

Fig. 4 shows the evolution of calculated band-gap as a function of the X electronegativity for the oxidized phases in reactions (1)–(3). The band-gap decreases with the stronger inductive effect with a linear dependence. In the $Li_yV^{+5}OXO_4$ [5] we found that the lower electronegative X ions will render more covalent M–O bond (shorter) enhancing the overlap of oxygen-2p and M-3d orbitals, therefore pushing the bonding O-p band downwards, and the antibonding TM-d bands upwards i.e. opening the band-gap. The electron donated during the lithium insertion is hosted in the antibonding TM d-states. As a bottom line, in $Li_yV^{+5}OXO_4$, the destabilization of the antibonding TM -3d states as we move towards less electronegative X has a twofold effect: widening the electronic band-gap and lowering the lithium insertion voltage. Interestingly, the evolution of the delithiated phases band-gaps and the calculated voltages with the X electronegativity shows opposite linear dependences in all the systems under study. Further investigation is in progress, in particular to explain why the band-gaps of lithiated and delithiated phases display an opposite trend as a function of the X electronegativity (compare Figs. 3 and 4).

Worth mentioning, in the view of Figs. 3 and 4, the compounds with higher band-gaps are those with a half closed-shell transition metal ions (Mn^{+2}, Fe^{+3}). For these ions, accepting an extra electron implies a high energy penalty; notice that the exchange energy gets its maximum value for the d^5 configurations. A direct consequence, is that lithium deinsertion is almost precluded from compounds based on Mn^{+2}, owing to the fact that a poor conductivity is expected in the electrode material and may be difficult to compensate even with carbon nano-coating of the particles. Yet some other conductivity mechanism as localized polarons could occur. This is in good agreement with the observation that the lithium deinsertion reaction is impeded from olivine-$LiMnXO_4$ (X = P, As), in contrast to what happens for olivine-$LiMXO_4$ with M = Fe and Co [8,20,25].

3.2. The Li_2MSiO_4 system

While only one electron per formula unit can be exchanged by lithium deinsertion from Li_yVOXO_4 (V^{+4}) and olivine-$LiMXO_4$ (Co^{+2}), it is in principle possible to fully extract lithium ions from Li_2MSiO_4, providing two electrons per formula unit (M^{+2}/M^{+3}, and M^{+3}/M^{+4} couples) [10]. Fig. 5 summarizes the calculated average lithium deinsertion voltage for the first lithium ion (reaction 3) together with that for the second lithium ion:

$$\square_2M^{+4}SiO_4 + Li \leftrightarrow \square LiM^{+3}SiO_4 \text{ and } (M = Mn, Fe, Co, Ni) \quad (4)$$

It can be observed that in all cases extraction of the second lithium ion will occur at very high voltages (>4.5 V), reaching the stability limit of the most used electrolytes for lithium batteries ($LiPF_6$ based) [26], hence the importance to move to ionic liquids that are more stable against

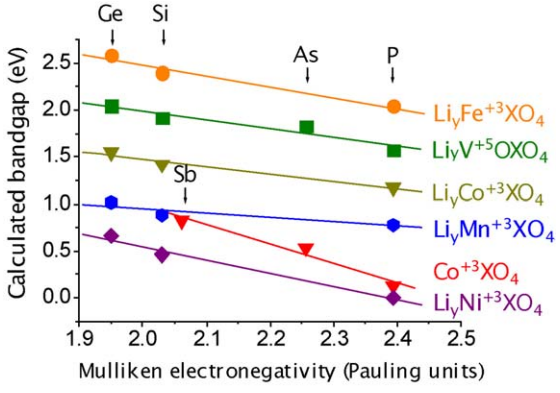

Fig. 4. Calculated band-gaps for $Co^{+3}XO_4$, $Li_yV^{+5}OXO_4$ and $Li_yM^{+3}XO_4$ compounds *vs.* the X Mulliken electronegativity. The lines show the fit to respective linear functions.

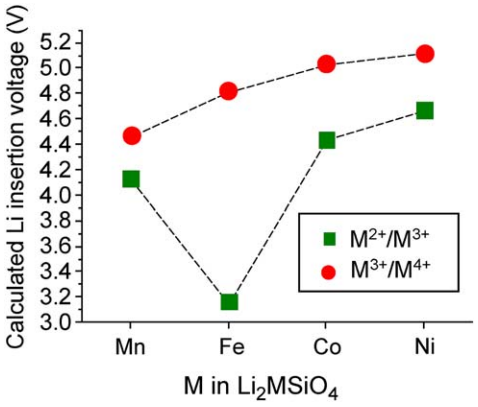

Fig. 5. Calculated lithium deinsertion voltages for the reactions $Li_2MSiO_4 \leftrightarrow LiMSiO_4 + Li$ (green squares) and $LiMSiO_4 \leftrightarrow MSiO_4 + Li$ (red circles).

oxidation (e.g., that can sustain higher voltages). Lithium deinsertion from Li_2FeSiO_4 will proceed in marked two step-voltage plateaus: a first at 3.2 V and a second at 4.8 V, with the voltage step of 1.6 V at the composition $LiFeSiO_4$. This huge jump is nested in the fact that we move from a d^6 ion (Fe^{+2}) to a closed-shell one, $d^5(Fe^{+3})$, that is requiring a small ionization energy as compared to the other 3d M^{+2} to M^{+3} oxidations. In Li_2MSiO_4 with M = Mn, Co and Ni the two voltage plateaus get closer, the predicted difference at 0 K being of about 0.5 V. Whether this voltage steps would be observed experimentally depends firstly on the stability of $LiMSiO_4$ towards disproportionation according to the following reaction

$$1/2Li_2MSiO_4 + 1/2\square_2MSiO_4 \leftrightarrow \square LiMSiO_4 \quad (5)$$

The formation energy of $LiMSiO_4$ can be obtained form a total energy expression, $E_f = E_t(LiMSiO_4) - 1/2\,E_t(MSiO_4) - 1/2E_t$ (Li_2MSiO_4). Fig. 6 shows the enthalpy of reaction (5) for M = Mn, Fe, Co and Ni. In all cases the formation energy is negative, indicating that $LiMSiO_4$is stable with respect to phase separation into Li_2MSiO_4 and $MSiO_4$ at low temperatures. The predicted stability for $LiFeSiO_4$ (0.83 eV) is in good agreement with the pronounced step in the experimental voltage–composition curve around that composition [27]. In the case of $LiMSiO_4$ with M = Mn, Co and Ni, the formation energy decreases to 0.16 eV, 0.3 eV and 0.2 eV, respectively. The high stabilization of the d^5 configuration certainly explains the different stability of $LiFeSiO_4$ compared to the others $LiMSiO_4$. To evaluate the stability of ordered $LiMSiO_4$ at non-zero temperature one has to account for the entropy. The temperature at which an ordered phase will disorder depends on the interactions between neighbor Li ions within a given host [28,29]. Obviously, for isostructural compounds, the electronic configuration of the transition metal ion also plays a role in the phase stability (compare for instance the Li_xCoO_2 [30] and Li_xNiO_2 [31] calculated phase diagrams). Though an investigation on the Li_xMSiO_4 phase stability will be needed to precise the temperature at which $LiMSiO_4$ will disorder, in principle, the Mn intermediate would be the most likely to disorder, maybe even at room temperature, thereby blurring out the voltage step in the voltage-composition curve. This would agree with experiments that show a smooth voltage–composition profile for Li_2MnSiO_4 compared to that of Li_2FeSiO_4 [10,12].

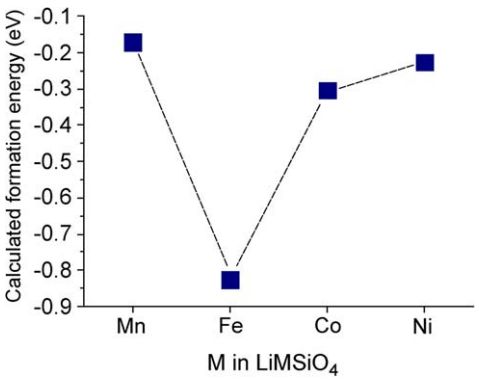

Fig. 6. Calculated formation energies of the $LiMSiO_4$ ordered structure (reaction 5) for different M.

Severe structural rearrangements are a major obstacle to topotactically remove lithium ions from a material (i.e. retaining the structural framework). Experimental and optimized unit cell parameters for Li_yMSiO_4 ($y = 0$, 1, 2) compounds are given in Table 1. The calculated lattice parameter of Li_2MSiO_4 are within 1.5% of experimental values (below 4% for volume predictions), which reflects again for the accuracy of the GGA + U method. A somewhat unexpected cell variation upon oxidation is observed for all Li_2MSiO_4 studied compounds, excepting for manganese. On the basis of the size reduction of M^{+2} ions when oxidized, one would expect a cell volume contraction. However, this is only observed for Li_2MnSiO_4 whereas for M = Fe, Co and Ni the cells expand. A detailed study of the optimized structures (not given) is needed to account for this. When comparing Li_2MSiO_4 and $MSiO_4$ structures the effect of the oxidation the M^{2+} ions to their tetravalent state results in a noticeable shortening of the M–O dis-

Table 1
Calculated lattice parameters (Å) for Li_xMSiO_4 compounds ($x = 0$, 1 and 2)

x		Mn	Fe	Co	Ni
2	***a***	6.3666 (6.3109)	6.3246 (6.271)	6.2015 (6.253)	6.2938
	b	5.4329 (5.3800)	5.3817 (5.338)	5.4378 (5.342)	5.3702
	c	5.0368 (4.9662)	4.9967 (4.9607)	4.9909 (4.929)	4.9137
	V	174.22 (168.61)	170.07 (166.05)	168.30 (164.66)	166.08
1	***a***	6.2641	6.0865	6.0706	5.9538
	b	5.4174	5.6326	5.5783	5.6453
	c	5.1527	5.0357	5.0428	4.9524
	V	174.86	172.63	170.77	166.45
0	***a***	6.1724	6.0676	5.9552	5.9492
	b	5.7043	5.6131	5.8102	5.6594
	c	4.8512	5.3032	5.0328	5.1399
	V	170.81	180.61	174.14	173.06

Experimental data are given in parentheses [10,37].

tances. Since along the ***a***-axis SiO_4 and MO_4 tetrahedra alternate by corner-sharing (Fig. 1) the shortening of the M–O bonds must be reflected in the contraction of the cell along this axis. On its hand, the Si–O distances remain virtually unchanged in the oxidized compounds, whereas the Si–Si distances slightly increase (by about 2%). Along the other two main directions some rearrangements of the structure occur. As observed in Table 1, the ***b***-axis considerably expands upon oxidation in all cases. From Fig. 1, it is evident that the lithium ions links the $[SiMO_4]_\infty$ layers together; therefore lithium extraction will weaken these forces and as result the layers will separate (and the ***b***-axis will expand), the cell enlargement along ***b*** ranging from 4% to 7% Nevertheless, the most important structural rearrangement occurs in the $[SiMO_4]_\infty$ corrugated layers. The degree of corrugation depends on the Si–O–M angles formed by SiO_4 and MO_4 tetrahedra sharing an oxygen atom to form chains running along the ***c***-axis (see Fig. 1). When lithium is extracted from Li_2MSiO_4 these layers become less corrugated since the Si–O–M angles open (get closer to 180°). As a result the ***c***-axis increases and the M–M and M–Si distances become larger, about 2% and 6%, respectively, allowing a minimization of strong cationic repulsions. For the manganese-containing compound the flattening of the $[SiMnO_4]_\infty$ layers is less pronounced than in the other cases, therefore this mechanism does not compensate the contraction of the Mn–O bonds, which is the predominant effect. Thus, the cell contracts along the ***c***-axis as well as along ***a***, giving a volume cell reduction of about 2%, instead of the volume expansion observed for the other $MSiO_4$ (M = Fe, Co and Ni) materials (ranging from 3% to 6%). In all cases, the fully delithiated $MSiO_4$ structures seem to be rather unstable, and we cannot discard that as Li is removed from Li_2MSiO_4 they might become thermodynamically metastable with respect to other structures. A good example of such structural phase transformation upon lithium removal is provided by the layered to spinel transformation that occurs in $LiMnO_2$ [32,33]. The shape of voltage–composition curve reported for the full lithium extraction from Li_2MnSiO_4 [12] suggests that an irreversible phase transformation may indeed occur at the end of the first charge. More experimental and/or computational work will be needed to verify this hypothesis.

In Li_2FeSiO_4 the possibility of reversibly extracting of more than one lithium ion is hindered by the high stability of the intermediate phase $LiFeSiO_4$. At this respect, Li_2MnSiO_4 seems to be a more promising material, consistently with some recent experimental reports [12]. The main drawback of Li_2MnSiO_4 would be its low electronic conductivity, as inferred form both experiments [12] and computational data. Li_2CoSiO_4 does not offer any improvement to Li_2MnSiO_4, but adds the disadvantage of a lithium intercalation voltage beyond reach in practice. Li_2NiSiO_4 with the lowest band-gap should not have the shortcoming of the Mn derivative. However, the predicted lithium intercalation voltages are also inconveniently high (4.67 V for the first Li and 5.12 V for the second). Nevertheless, the voltage could possibly be lowered taking advantage of the inductive effect by partially substituting silicon by another suitable element to obtain $Li_zNiSi_{1-y}X_yO_4$ compounds. The electronegativity of Si is 2.03, and less electronegative substitutes could be Al^{+3} (1.37) and Ti^{+4} (1.28 from Allen [15]). Both choices are rather judicious as the existence of alumino-silicates and compounds, where Ti^{+4} ions occupy tetrahedral sites [34–36] are well documented. Precise lithium intercalation voltages for $Li_2NiSi_{1-y}Ti_yO_4$ can be extracted from Fig. 2; using the corresponding linear fit (purple line) the lithium intercalation voltage of $Li_2Ni^{+2}Si_{0.5}Ti_{0.5}O_4$ is extrapolated to be 4.50 V. For the shake of completeness we went into the exercise of doing such a calculation, getting a voltage of 4.58 V in good agreement with extrapolated value. This confirms the usefulness of the voltage–electronegativity correlations to rapidly estimate voltage values for a particular XO_4 polyoxianion group within a given structural type/redox couple.

Some words must be devoted to the coordination polyhedra of TM ions in delithiated Li_2MSiO_4. Our results are obtained within the Li_2MSiO_4 host, therefore keeping the TM ions in tetrahedral sites. However, much caution must be exercised due to the known tendency of a given TM ion (with its corresponding electronic configuration) to occupy specific oxygen environments. Thus, while tetravalent iron in tetrahedral coordination is not so scarce, materials with tetrahedrally coordinated Mn^{4+} or Co^{4+} are a rarity and, to our knowledge, there is no compound with tetravalent nickel in such a tetrahedral environment. Obviously, there is a strong driving force for the TM ions to change the coordination upon lithium extraction and the structure of $MSiO_4$ to transform into a more stable new structure or to collapse. This is the main drawback of this family of orthosilicates.

4. Conclusions

In the last decade the ability of first principles calculations to guide the search for promising electrode materials has been widely demonstrated. In this work we show that for polyoxianionic compounds possessing XO_4 groups, the calculated lithium intercalation voltage correlates to the Mulliken X electronegativity, displaying a linear dependence for each *structural type/redox couple*. Experimental lithium insertion voltages already available in the literature support these results. The systematic mapping of such a voltage to electronegativity correlations allows the design on demand of novel polyoxianionic compounds as cathode for lithium batteries. Needless to say that some of these hypotheses are being experimentally tested.

Acknowledgement

This work was supported by CICYT (MAT2004-03070-C05-01) and CAM (Project S-0505/PPQ-0093). MEAD

wants to thanks the Spanish MEEC for RC contract. Valuable comments from E. Moran are highly appreciated. Authors are grateful to CIEMAT Supercomputing Centre for access to the jen50 SGI.

References

[1] A.K. Padhi, A.K. Nanjundaswamy, C. Masquelier, S. Okada, J.B. Goodenough, J. Electrochem. Soc. 144 (5) (1997) 1609.
[2] A.K. Padhi, K.S. Nanjundaswamy, J.B. Goodenough, J. Electrochem. Soc. 144 (4) (1997) 1188.
[3] A.K. Padhi, K.S. Nanjundaswamy, C. Masquelier, J.B. Goodenough, J. Electrochem. Soc. 144 (8) (1997) 2581.
[4] C. Masquelier, S. Patoux, C. Wurm, M. Morcrette, in: G. Nazri, G. Pistoia (Eds.), Lithium Batteries: Science and Technology, Kluwer Academic Publishers., Dordrecht, 2004.
[5] M.E. Arroyo-de Dompablo, M. Morcrette, J.M. Tarascon, submitted for publication.
[6] M.E. Arroyo de-Dompablo, M. Morcrette and J.M. Tarascon, Abstract 357, IMLB, June 18–23, Biarritz, France, 2006.
[7] A.S. Prakash, P. Rozier, L. Dupont, H. Vezin, F. Sauvage, J.M. Tarascon, Chem. Mater. 18 (2) (2006) 407.
[8] M.E. Arroyo-de Dompablo, U. Amador, F. Garcia-Alvarado, J. Electrochem. Soc. 153 (4) (2006) A673.
[9] M. Armand et al, World Patent WO02/27823, 2002.
[10] R. Dominko, M. Bele, M. Gaberscek, A. Meden, M. Remskar, J. Jamnik, Electrochem. Commun. 8 (2) (2006) 217.
[11] A. Nyten, A. Abouimrane, M. Armand, T. Gustafsson, J.O. Thomas, Electrochem. Commun. 7 (2) (2005) 156.
[12] Y. Yang, Y. Li, Z. Gong, Abstract 210, IMLB, June 18–23, Biarritz, France, 2006.
[13] H. Arrabito, N. Penazzi, S. Panero, P. Reale, J. Power Sources 94 (2, 10) (2001) 225.
[14] P. Millet, C. Satto, Mat. Res. Bull. 33 (9) (1998) 1339.
[15] L.C. Allen, J. Am. Chem. Soc. 111 (25) (1989) 9003.
[16] P.E. Bloch, Phys. Rev. B 50 (1994) 17953.
[17] G. Kresse, J. Joubert, Phys. Rev. B 59 (1999) 1758.
[18] G. Kresse, J. Furthmuller, Comp. Mat. Sci. 15 (1996) 6.
[19] F. Zhou, M. Cococcioni, C.A. Marianetti, D. Morgan, G. Ceder, Phys. Rev. B 15 (2004) 235121.
[20] F. Zhou, M. Cococcioni, K. Kang, G. Ceder, Electrochem. Commun. 6 (11) (2004) 1144.
[21] M.K. Aydinol, A.F. Kohan, G. Ceder, K. Cho, J. Joannopoulos, Phys. Rev. B 56 (3) (1997) 1354.
[22] F. Zhou, K.S. Kang, T. Maxisch, G. Ceder, D. Morgan, Solid State Commun. 132 (3–4) (2004) 181.
[23] F. Zhou, C.A. Marianetti, M. Cococcioni, D. Morgan, G. Ceder, Phys. Rev. B 69 (2004) 201101(R).
[24] T. Maxisch, F. Zhou, G. Ceder, Phys. Rev. B 73 (2006) 104301.
[25] C. Delacourt, P. Poizot, M. Morcrette, J.-M. Tarascon, C. Masquelier, Chem. Mater. 16 (1) (2004) 93.
[26] P. Guyomard, J.M. Tarascon, J. Electrochem. Soc. 140 (11) (1993) 3071.
[27] A. Nytén, T. Gustafsson, J. Thomas, M. Armand, R. Dominko, M. Gaberscek, J. Jamnik, Abstract 213 IMLB, June 18–23, Biarritz, France, 2006.
[28] W.R. McKinnon, in: P. Bruce (Ed.), Solid State Electrochemistry, Cambridge University Press, Cambridge, 1995.
[29] G. Ceder, A. Van der Ven, Electrochem. Acta 45 (1–2) (1999) 131.
[30] A. Van der Ven, M.K. Aydinol, G. Ceder, G. Kresse, J. Hafner, Phys. Rev. B 58 (6) (1998) 2975.
[31] M.E. Arroyo-de Dompablo, A. Van der Ven, G. Ceder, Phys. Rev. B 66 (6) (2002) 064112.
[32] J. Reed, G. Ceder, A. Van Der Ven, Electrochem. Solid State Lett. 4 (6) (2001) A78.
[33] A.R. Armstrong, P.G. Bruce, Nature 381 (1996) 499.
[34] B.M. Gatehouse, Acta Crystallogr. C45 (3) (1989) 1674.
[35] J.R. Günter, G.B. Jameson, Acta Crystallogr. C40 (11) (1984) 207.
[36] N.M. Bobkova, E. Rachkovskaya, J. Appl. Spectrosc. 24 (2) (1976) 196.
[37] H. Yamaguchi, K. Akatsuka, M. Setoguchi, Y. Takaki, Acta Crystallogr. B35 (1979) 2680.